Available online at www.sciencedirect.com
ScienceDirect
Electrochimica Acta 53 (2007) 1432–1438
ELECTROCHIMICA Acta
www.elsevier.com/locate/electacta

Electrochemical behavior of lithium intercalated in a molybdenum disulfide-crown ether nanocomposite

M.A. Santa Ana [a], N. Mirabal [a], E. Benavente [b], P. Gómez-Romero [c], G. González [a,*]

[a] *Department of Chemistry, Faculty of Sciences, Universidad de Chile, Casilla 653, Santiago, Chile*
[b] *Department of Chemistry, Universidad Tecnológica Metropolitana, Av. José Pedro Alessandrri 1242, Santiago, Chile*
[c] *Instituto de Ciencia de Materiales de Barcelona (CSIC), Campus UAB, 08193 Bellaterra, Barcelona, Spain*

Received 20 December 2006; received in revised form 25 April 2007; accepted 16 May 2007
Available online 2 June 2007

Abstract

A new nanocomposite, obtained from the intercalation of the cyclic ether 12-Crown-4 into MoS_2, $Li_{0.32}MoS_2(12\text{-Crown-4})_{0.19}$, is described. The laminar product has an interlaminar distance of 14.4 Å. The electrical conductivity of the nanocomposite varies from 2.5×10^{-2} to 4.3×10^{-2} S cm^{-1} in the range 25–77 °C, being about four times higher than the analogous poly(ethylene oxide) (PEO) derivative at room temperature. The electrochemical step-wise galvanostatic intercalation or de-intercalation of lithium, leading to $Li_xMoS_2(12\text{-Crown-4})_{0.19}$ with x in the range 0.07–1.0, indicates a Li/Li$^+$ pair average potential of 2.8 V. The electrochemical lithium diffusion coefficients in the crown ether intercalates, determined by galvanostatic pulse relaxation between 15 and 37 °C at different lithium intercalation degrees, are higher than those of the PEO derivatives under similar conditions, being however the diffusion mechanism rather more complex. The variation of both, the lithium diffusion activation enthalpy and the quasi-equilibrium potentials, with the lithium content shows there are two different limit behaviors, at low and high lithium intercalation degree, respectively. These features are discussed by considering the high stability of the Li-crown ether complex and the different chemical environments found by lithium along the intercalation process.

Keywords: Molybdenum disulfide; Lithium intercalation; Lithium-ion activity; Crown ether; Laminar organic–inorganic nanocomposites

1. Introduction

Layered compounds may be in general considered as micro heterogeneous entities formed by two interpenetrated phases. A rigid phase, formed by molecular or atomic species held together by strong ionic-covalent bonds bearing to two-dimensional sheets, and a much more flexible phase constituted by the interlaminar surfaces defined by the former. Since the interactions between the rigid laminae or among the species there being in the interlaminar spaces are in general weak, the intercalated phase is in general more fluid and labile to react with the medium. The rich intercalation chemistry, characteristic for layered compounds, is therefore essentially determined by the changes in the nature of the interlaminar phase, remaining the host rigid structure practically unaltered [1].

Ionic conductivity in solids is known to be strongly dependent on the magnitude and the flexibility of the force field at the position occupied by the charge carrier in the equilibrium state, decreasing with the height of the energy barrier to the charge movement. Comparing the conventional ionic-covalent structures of inorganic solids with those of the interlaminar phases in layered solids, the scenario for the migration of ions is certainly much favorable in the latter where there is a quasi liquid state. Under such conditions fast ionic conductivity could be expected [2].

The intercalation of metal ions into layered isolators like clays normally occurs by ion exchange [3]. However, in the case of layered conductors or semiconductors, the intercalation may be performed from the metal or from a compound

* Corresponding author.
E-mail address: ggonzale@uchile.cl (G. González).

0013-4686/$ – see front matter © 2007 Elsevier Ltd. All rights reserved.
doi:10.1016/j.electacta.2007.05.059

with the metal in a low oxidation state in a process generally associated to a charge transfer from the inserted species to the rigid host [4,5]. Depending on the magnitude of the charge transfer, the metallic species inserted in the interlaminar phase presents a normal or a fractional oxidation state [6]; thus the rigid phase is converted in a polyanionic host allowing the solid to behave as mixed electronic-ionic conductor [7]. These products are specially appropriated as electrode materials, where both electron and ion transport have to be optimized.

Most studies on layered mixed conductors refer to the intercalation of lithium. The electronic configuration, the low atomic weight and the potential of the Li/Li^+ pair, make this element particularly relevant in the development of high potential electrochemical cells and batteries [8]. From such a point of view it is interesting to analyze the influence of the modification of the laminar phase by the intercalation of organic donors on the properties of intercalated lithium, especially on the potential of the Li/Li^+ pair on the lithium diffusion. Resulting nanocomposites are also important due to the variety of combinations and the manifold of synergic effects they made induce, opening the possibility of designing products useful as tuneable, tailor-made materials [9–12]. Beyond their potential applicability, this chemistry is also important from the point of view of basic knowledge. Indeed it may contribute to answer fundamental chemical questions – like molecular recognition and self-assembling – related to host–guest and guest–guest interactions leading to the genesis of these microheterogeneous species as well as to the effects they cause on electronic and conformational properties of the constituting phases.

During the last years we have been interested in the intercalation chemistry of molybdenum disulfide [13]. This lamellar solid is a semiconductor constituted by MoS_2 layers which in the pristine molybdenite are formed by a layer of molybdenum atoms sandwiched by two layers of sulfur atoms in a trigonal prismatic configuration. In the intercalated state the molybdenum atoms are however located in octahedral sites, that corresponding, according to its electronic band structure description, to an electronic conductor [14]. Our approach in this chemistry refers principally to investigate the effect of the co-intercalation of lithium and electron pair donors on the electrical and electrochemical properties of the products [13]. Especially interesting is the case in which the mobile interlaminar phase is formed by the co-intercalation of lithium and a polymer widely used in solid ionic conductors, the poly(ethylene oxide) (PEO), a combination inducing a clear improvement of both electronic and ionic conductivity [7,15–18]. Interesting results have been also obtained with the nanocomposite MoS_2-poly(acrylonitrile) leading to products with a Li/Li^+ pair average potential of 2.85 V, and a lithium diffusion coefficient of about 4×10^{-11} cm^2 s^{-1} at room temperature. In order to investigate the effect of the stabilization of the lithium ion in the interlaminar space we have selected a ligand with an especially high affinity for this ion. Thus, in this work we specifically describe the electrical conductivity of the product arising from the co-intercalation of lithium and 12-Crown-4 ether as well as the effect of the amount of intercalated lithium on both the mobility and activity of lithium ion in the intercalates.

2. Experimental

2.1. Synthesis and characterization

To a suspension of 0.5 g de Li_xMoS_2 (prepared by treating MoS_2, 99% <2 μm, Aldrich, with 1.6 M *n*-butyllithium, in *n*-hexane, Merck, under argon atmosphere) were added 0.4 ml of 12-Crown-4 Aldrich, 98%. The reaction mixture was stirred during 24 h at room temperature under argon atmosphere. The black solid product separated by centrifugation was twice washed with dry *n*-hexane, dried at the air, washed again with water and finally dried under vacuum. The product was characterized by elemental analysis (C, H, N, S elemental combustion analysis, SISONS Model EA-1108 analyzer); atomic absorption spectroscopy for Li (UNICAM 929, λ 670 nm), powder X-ray diffraction analysis (Siemens D-5000 diffractometer, Cu Kα radiation), and thermal gravimetric analysis (simultaneous TG-DTA Netzch STA 409, argon, heating rate of 10 °C min^{-1}). Analysis: found (calculated for $Li_{0.32}MoS_2$(12-Crown-4)$_{0.19}$): C 9.08 (9.11), H 1.26 (1.53), S 32.1 (32.9), Li 1.16 (1.14).

2.2. Electrical and electrochemical measurements

The electrical conductivity of the product at several temperatures in the range 25–77 °C was measured by electrochemical impedance spectroscopy (EIS) (Autolab PGSTAT12 with FRA2 module), using pressed samples between ion-blocking gold electrodes. The electrical conductivity (σ) was calculated from resistance $R = [Z']$ in the impedance spectra $Z = Z' + iZ''$ by $\sigma = l/RA$ where l is the thickness and A the area of the sample.

Compounds with different lithium content were obtained electrochemically, by step-wise galvanostatic intercalation (or deintercalation) in the electrochemical cell – Li/1 M $LiClO_4$ in a (1:1) ethylene carbonate–propylene carbonate solution/$Li_{0.32}MoS_2$(12-Crown-4)$_{0.19}$ – at a current density of 150 μA cm^{-2}, using a Pontentiostat-Galvanostat PARC model 175. The cathode, consisting in a 6.6 mm diameter compacted pellet of the sample, and a piece of 7.5 mm thin lithium ribbon, acting both as anode and reference electrode, were separated by a glass fiber soaked in a 1 M $LiClO_4$ electrolytic solution. Cells were built up in a dry argon-filled glove box and kept hermetically sealed during the experiments. Charge or discharge experiments were performed at room temperature. The amount of intercalated lithium was determined coulommetrically after each galvanostatic step. Quasi equilibrium potentials measured for each step – 1 h intercalation followed by 11 h rest under open circuit conditions – were referred to the Li/Li^+ electrode.

Chemical diffusion coefficients were determined in the same cell by the galvanostatic pulse relaxation technique [19] at several temperatures in the range 15–37 °C and at different lithium intercalation degrees.

3. Results and discussion

3.1. Synthesis

The intercalation of electron pair donors into molybdenum disulfide is widely known [13,20]. Also the intercalation of cyclic ethers has been informed previously [21]. In most cases the synthesis method considers the activation of the pristine molybdenum disulfide by lithium intercalation followed by a rapid hydrolysis of the lithiated product [22]. By this way the sulfide undergoes an exfoliation process that, in addition to a mechanical activation, produces a chemical activation by the conversion of the MoS_2 from its original trigonal prismatic conformation to an octahedral one as well as the partial reduction of the sulfide matrix. Thus, the reaction of exfoliated $LiMoS_2$ with the crown ether spontaneously forms the nanocomposite $Li_{0.32}MoS_2(12\text{-Crown-4})_{0.19}$ at room temperature. The product shows a rather high stability, being indeed stable for more than a week at the air as well as in water, one of the solvents used for removing reagent excesses.

The product is a single layered phase, however it is obtained as microcrystalline powder formed by platelets about 3 nm thick and 200 nm diameter, being the system intrinsically anisotropic. The transport of electrons and ions that occurs along the MoS_2 layers and the interlaminar phase, respectively, is always higher along the direction parallel to the laminar plane of the platelets than along the perpendicular one. In a microcrystalline sample the properties should ideally correspond to an average of all possible directional contributions; however, some degree of macroscopic anisotropy is frequently induced during the preparation of the sample. Indeed, the anisotropy of MoS_2 as well as of its intercalates may be regulated in some extend by pressing the microcrystalline powder [23,24], that induces more platelets being preferentially oriented with the laminar plane perpendicular to the pressure direction. The samples for the electrical conductivity and lithium diffusion measurements described below were prepared by pressing the microcrystalline powder in the form of disks, which were then used oriented perpendicularly to the transport direction. Though the pressure used for compacting the microcrystalline sample was relatively low (about 500 MPa) results reported below are therefore expected to be always slightly lower than those expected for ideal microcrystalline specimens.

3.2. Structure and stoichiometry

The X-ray analysis of the product illustrated in Fig. 1 indicates the formation of a pure layered phase with an interlaminar distance of 14.4 Å. This distance – which corresponds to an increase of about 8.3 Å respect to that observed for MoS_2 either pure or intercalated with lithium – agrees well with the molecular structure of the isolated crown ether which can be seen as a cylindrical body of 2.5 Å length and 6.2 Å diameter (Scheme 1). Such a model, based on a geometrical criterion [25,26], may be also used for understanding the stoichiometry of the product. If we consider that the surface available in the MoS_2 interlamellar spaces is about 8.6 $Å^2$ per molybdenum atom as well

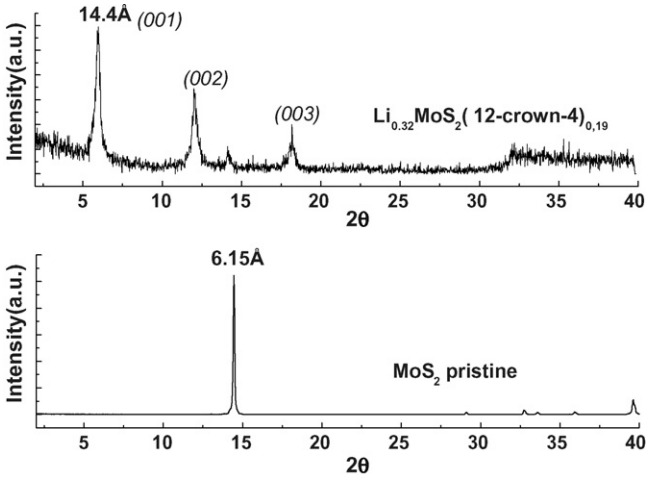

Fig. 1. Powder X-ray diffraction patterns of the nanocomposite $Li_{0.32}MoS_2(12\text{-Crown-4})_{0.19}$ (top) and pristine MoS_2 (bottom).

as that each ether molecule, assuming it can rotate around its own axis at room temperature, occupies a surface of about 6.2 Å × 6.2 Å; then the maximal amount able to be intercalated in the interlamellar spaces should be about 0.22 ether molecules per molybdenum atom. This value is not very different from the 0.19 mol 12-Crown-4 per mol MoS_2 observed experimentally. Moreover, it is also interesting to comment the relatively high amount of lithium, 0.32 mol per mol MoS_2, retained in the nanocomposite. The lithium contents reported for other chemically intercalated MoS_2 products obtained by a similar procedure are generally lower. For exfoliated MoS_2 as well as for the PEO and secondary amines derivatives values around 0.1 are observed [2,26,17]. The role of lithium in these intercalates is to maintain the charge balance in the system counteracting the residual negative charge generated in the MoS_2 matrix during the intercalation process that accounts for the stabilization of the octahedral configuration in the products. Considering that the stability of the lithium ion in the presence of a specific ligand like 12-Crown-4 ether ($K_S \approx 10^4$ [27]) is higher than forming

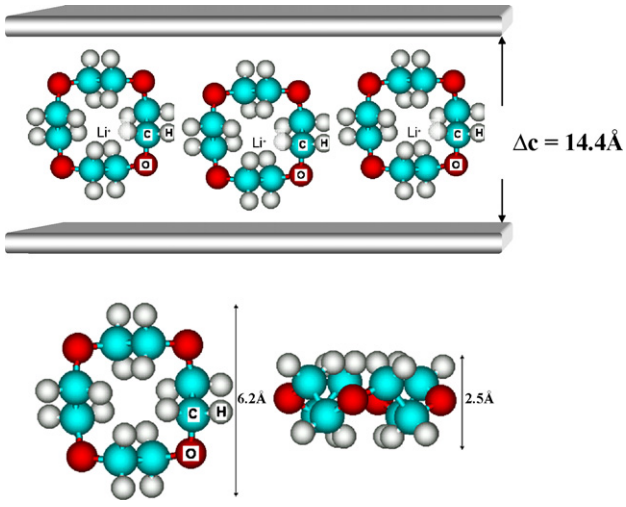

Scheme 1. Van der Waals radii molecular model of the 12-Crown-4 free and intercalated in MoS_2.

Table 1
Comparison of the structural, electrochemical and conductivity properties between molybdenum disulfide nanocomposite with crown ether and poly(ethylene oxide) [29]

Compound	Interlamellar distance (Å)	Average potential (V vs. Li/Li$^+$)	σ at 298 K (S cm^{-1})
$Li_{0.32}MoS_2$(12-crown-4)$_{0.19}$	14.4	2.80	2.85×10^{-2}
$Li_{0.1}MoS_2(PEO)_1$	16.3	2.60	6.60×10^{-3}
$Li_{0.1}MoS_2(PEO)_{0.5}$	11.6	2.78	4.80×10^{-4}
MoS_2	6.15	1.60	2.10×10^{-6}

complexes with more simple ligands like the linear polyethers, we can state that the higher content of lithium indicates a greater excess of negative charge in the MoS_2 sheets.

3.3. Electrical conductivity

Although the MoS_2/donor/Li composites are mixed electron-ion conductors, the ionic conductivity is about 10^{-4} to 10^{-5} lower than the electronic one [2,7,24]. Reported electrical conductivity values refer therefore mainly to the electron transport taking place in the individual MoS_2 layers. Since results refer to microcrystalline solid, at least two important contributions to conductivity, the intrinsic conductivity on the individual grains or platelets and the intergrain conductivity should be considered.

The solid behaves as an electrical semiconductor with conductivities between 2.5×10^{-2} and 4.3×10^{-2} S cm^{-1} in the studied temperature range, Fig. 2. Although the observed conductivity is rather higher than for the pristine MoS_2, the behavior as an electronic conductor expected for intercalated MoS_2 with an octahedral conformation is not observed. However, this positive dependence of the conductivity on the temperature in our product is qualitatively similar to those observed for other MoS_2 organic-inorganic nanocomposites [2,7]. Such an apparently anomalous behavior probably arises from the microcrystalline nature of the solid in which the barrier to electron transport probably is significantly influenced by the intergrain resistance to the electron flow between the disordered platelets. Furthermore, that barrier is probably also enhanced by the organic layer inserted between the conducting inorganic molecular sheets [23]. Because of the complexity of the intergrain processes, any analysis has to be limited to the intrinsic conductivity.

The comparison of the electrical conductivities at room temperature reported in Table 1 indicates that the crown ether derivative is about four times better conductor than the poly(ethylene oxide) (PEO) intercalates. Since the electron transport occurs in the MoS_2 layers, it is expected the electron mobility be independent on the nature of the interlaminar phase. However differences in the intrinsic conductivity between the crown and the PEO nanocomposites can be expected because of the carrier concentration in the MoS_2 layers, which as discussed above appears to be higher in the crown ether nanocomposite than in the PEO one. Although the "energy barrier" to the electron flow could be approximately estimated from the curve in Fig. 2, the complex nature of this barrier, which as discussed above should correspond to a compromise between the intrinsic conductivity of the layers and the dielectric effect of the organic component in the interlaminar space, discourages any further discussion of this parameter.

3.4. Lithium-ion diffusion

The variation of the lithium diffusion coefficients with the amount of intercalated lithium and with the temperature is illustrated in Fig. 3. As observed, the Arrhenius plots are linear

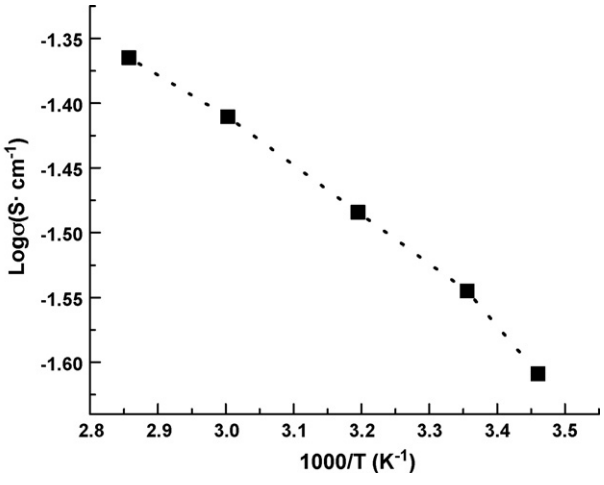

Fig. 2. Arrhenious plot for the electrical conductivity of the nanocomposite $Li_{0.32}MoS_2$(12-Crown-4)$_{0.19}$.

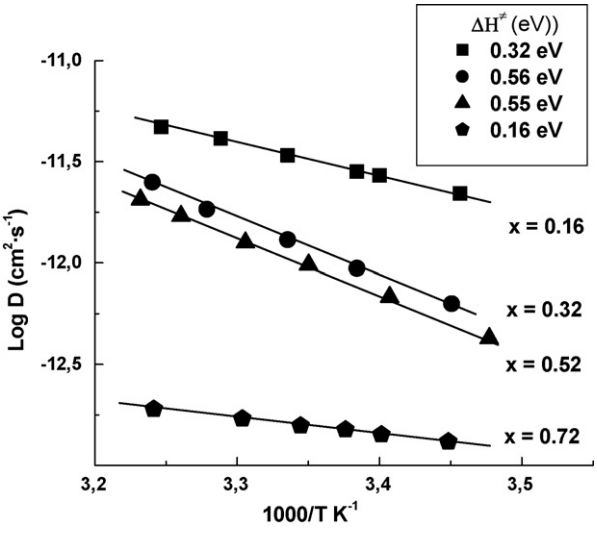

Fig. 3. Arrhenious plots describing the dependanse of the lithium diffusion coefficients in nanocomposites Li_xMoS_2(12-Crown-4)$_{0.19}$ on both temperature and lithium content (x). In the insert, values for the corresponding activation enthalpies ($\Delta H^{\neq}$) estimated from the slopes of the curves.

in the working temperature range, independently of the concentration of lithium in the sample. However the slopes of the curves are different. For samples with low lithium concentration $x = 0.16$–0.32, the lithium diffusion activation enthalpy increases with x while for samples with large x values $x = 0.52$–0.72, the opposite effect is observed. In the middle x-range both effects seem to be compensated and small changes of the activation enthalpy with the amount of lithium are observed. This rather complex behavior is characteristic of the crown ether nanocomposite, being not observed for lithium intercalated neither in MoS_2 nor in other MoS_2 organic–inorganic nanocomposites previously investigated [17]. The peculiarities of this system will be discussed further below, in the section "Interlaminar Phase Structure and Lithium Ion Properties."

3.5. Lithium/lithium-ion potentials

The variation of the of nanocomposite Li/MoS_2/Crown ether Li/Li^+ potential with the amount of intercalated lithium is reported in Fig. 4, together with those previously reported for the MoS_2 and its PEO derivative [28]. The regulation of the amount of lithium in the process described in Fig. 4 is performed electrochemically starting from the nanocomposite $Li_{0.32}MoS_2(12\text{-Crown-4})_{0.19}$ prepared by chemical intercalation. As can be observed in the figure, the lithium de-intercalation process leads to slight positive changes in the cell potential reaching a maximum at $x = 0.22$. However, in the opposite direction, lithium intercalation, the potential fall off rapidly. The high potential values observed in the first part of the curve ($x \leq 0.32$) agree with the expected stabilization of the lithium ion in the interlaminar phase arising from the high formation constant of the Li-12-Crown 4 complex [27]. For the same reason, the potentials for the crown ether intercalate are in general higher than that for the linear ether PEO, with average potentials of 2.8 V and 2.61 V, respectively. Although the potential behavior at low lithium content for both ether derivatives is qualitatively similar, they clearly differ when the lithium content is high, showing the crown ether nanocomposite a potential decay more abrupt, in a manner qualitatively similar to that observed for the MoS_2. These features indicate that in the variation of the potentials with the lithium content there are at least two different behaviors observable respectively at low and high lithium concentration. This phenomenon will be further discussed together with the qualitatively similar trends observed for lithium diffusion activation enthalpy in the next section.

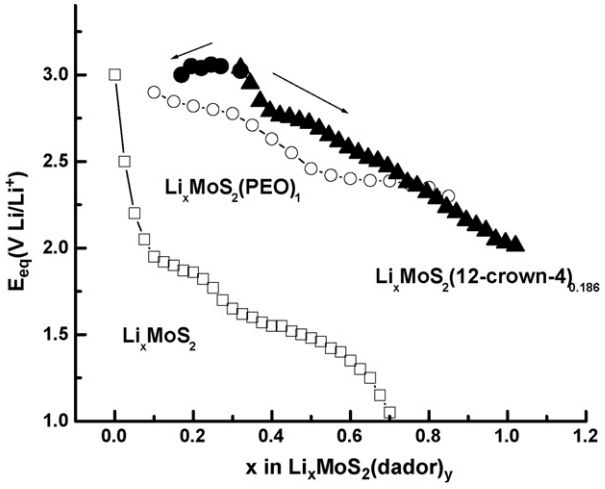

Fig. 4. Variation of the quasi-equilibrium potentials of nanocomposites $Li_xMoS_2(12\text{-Crown-4})_{0.19}$ (● for deintercalation and ▲ for intercalation) with lithium intercalation degree compared with those of the nanocomposites $Li_xMoS_2(PEO)_{1.0}$ (◯) and of Li_xMoS_2 (□).

3.6. Interlaminar phase structure and lithium-ion properties

The activity of lithium ion in the intercalation compounds depends principally on two factors: The chemical potential of the electron in the host and the chemical potential of the lithium ion in the interlaminar phase, being the latter determined by the chemical neighborhood of lithium especially by its inner coordination sphere. If we assume that the potential of the Li/Li^+ pair may be considered to be a measure of the lithium-ion activity, the curves in Fig. 4 would be a qualitative description of the dependence of the lithium-ion activity on the lithium concentration in the nanocomposite. In such a context it is interesting to realize that this activity reaches a maximum at about $x = 0.22$, not far from the value 0.19 corresponding to a stoichiometric ratio Li:(12-Crown-4) 1:1 in the nanocomposite. Thus, the formation of the complex of lithium with the crown ether appears to be the predominant factor in the stabilization of the lithium ion in the interlaminar phase. The excess of lithium, when the intercalation goes beyond this stoichiometry, should have a different coordination sphere leading to a lower stability of the lithium ion and to a decrease of the cell potential. Given the relatively dense arrangement of the crown ether molecules in the nanocomposite interlaminar space (Scheme 1), the excess of lithium is expected be mainly located near the host sulfur layer. Such an interpretation permits to understand the shape of the curve potential versus x in Fig. 4 which at high lithium concentration is similar to that of the MoS_2. The changes in the inner coordination sphere of lithium with the intercalation degree should be also reflected in the variation of the lithium diffusion coefficients commented before. In general, diffusion rates are determined by the free energy necessary for the lithium species passing through a high energy state in its transit between two low energy equivalent sites. In the intercalation compounds, the activation entropy changes associated to the lower availability of vacant sites for lithium diffusion is the predominant contribution to that activation energy. Thus, at a given temperature the diffusion coefficients normally decreases with increasing lithium content as occurs in our case. The enthalpy contribution to the activation free energy essentially depends on the relative energy of the ground and the exited states, i.e. on the neighborhood of the lithium ion in the sites corresponding to these states. This contribution is therefore sensitive to the structural and mechanistic changes occurring along the lithium intercalation. In cases like the intercalation of lithium into MoS_2 and the MoS_2/PEO nanocomposites, simple relationships of the activation enthalpy with the amount of intercalated lithium are observed. Thus for

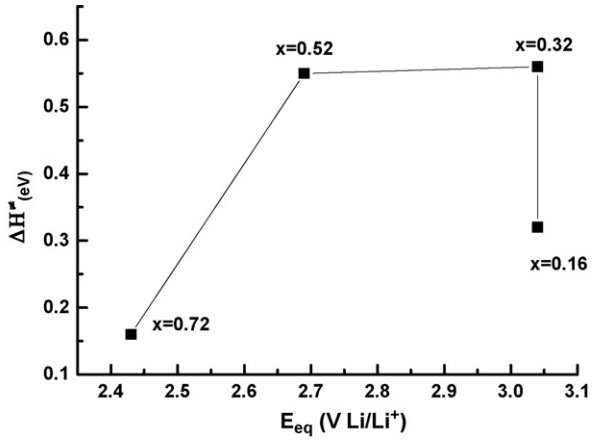

Fig. 5. Graphical comparison of lithium-ion activity, expressed by the Li/Li^+ quasi-equilibrium potentials, with the lithium diffusion activation enthalpies in the nanocomposites $Li_xMoS_2(12\text{-Crown-4})_{0.19}$ at different lithium intercalation degrees.

Li_xMoS_2, $\Delta H^{\neq}$ is totally independent on lithium concentration and for the nanocomposites $Li_xMoS_2(PEO)_1$, $\Delta H^{\neq}$ varies slowly and linearly with x. That contrasts with the non-linear behavior of the activation enthalpy for the (12-Crown-4) derivative described before, for which two different, opposite trends at low and high lithium content respectively, are observed.

In Fig. 5 the values of $\Delta H^{\neq}$ are graphically compared with the respective electrochemical intercalation potentials; the two limit behaviors commented above are apparent: one at low lithium concentration, when lithium is mainly located in the cyclic ether tetrahedral cavity, where the activation enthalpy increases while the lithium-ion activity, remains practically invariant. The other, at high lithium concentration, where lithium experiences the proximity not only of the crown ether but also of the neighboring MoS_2 sulfur atoms, the activation enthalpy decreases together with the lithium-ion stability.

The dependence of the diffusion activation enthalpy on lithium concentration may be interpreted in our case as a play between the relative energy of both ground and excited state of lithium involved in the ion-hopping diffusion mechanism. At low lithium concentration the coordination of lithium ion by the crown ether stabilizes strongly the ground state, making it insensitive to the concentration of the lithium ion. The activation enthalpy in this concentration range should be then determined by the relative energy of the lithium ion in the excited state, which appears to be influenced by the charge transferred to the sulfide matrix during the intercalation process. In the high lithium concentration range, where an important part of the lithium undergoes more directly the effect of the MoS_2 sulfur atoms, the lithium activity and the ground state stability decreases with increasing lithium concentration, thus lowering the activation enthalpy. The determinant factor in this range should be then the relative energy of the lithium ion in the ground state, decreasing the activation enthalpy together with the decrease of the lithium-ion activity. Cooperative effects between these two limit mechanisms would be the responsible of the relatively high activation enthalpy observed in the medium lithium intercalation range.

4. Conclusions

The intercalation of 12-Crown-4 into molybdenum disulfide leads to the nanocomposite $Li_xMoS_2(12\text{-Crown-4})_{0.19}$ with an interlaminar distance of 14.4 Å in which lithium appears to be coordinated by the intercalated ether molecules with their molecular planes oriented perpendicularly to the MoS_2 layers. The strong capacity of the ligand 12-Crown-4 to stabilize lithium ion induces the formation of a product with a relatively high lithium content which shows an electrical conductivity higher than the derivatives with linear polyethers.

The effect of the strong and near quantitative coordination of lithium by the intercalated 12-Crown-4 is also reflected in the electrochemical properties of the product. Nanocomposites with stoichiometries $Li_xMoS_2(12\text{-Crown-4})_{0.19}$ with x in the range 0.07 to 1.0 are obtained by electrochemical lithium intercalation/de-intercalation processes. The average potential of the Li/Li^+ pair in these products is 2.8 V. The variation of the quasi/equilibrium potentials with the amount of intercalated lithium, x, indicates however that two different processes at low and high lithium content respectively are apparent. These processes are determined by the amount of intercalated crown ether. Thus the potential, which remains practically unaltered in the range of x around or below the stoichiometry of Li in the 12-Crown-4 1:1 complex ($x = 0.19$), decreases rapidly beyond this molar ratio, i.e. when in the vicinity of lithium may be found not only the crown ether molecule but also the matrix sulfur atoms.

The electrochemical lithium diffusion coefficients in the crown ether intercalates are always higher than in the derivative with a linear polyether under similar conditions; moreover, the diffusion mechanism is rather more complex. The lithium diffusion activation enthalpies vary with the amount of intercalated lithium in a non-linear way being observed two limit behaviors at low and high lithium content respectively. Such a behavior may be understood by the influence of the vicinity of lithium in the interlaminar phase on the relative energies of the basal and/or activated complexes involved in a hopping lithium diffusion mechanism.

Comparing the charge discharge curves for the crown ether nanocomposite described here with those of other donors like PEO (Fig. 4) or poly(acrylonitrile) [29], we realize that the latter, due to smaller variation of the potential during the process, are more appropriate as battery electrodes than the former. However, the relatively high lithium diffusion rates together with the notorious potential changes produced in a relatively short lithium concentration range observed for the crown ether derivative might be interesting as material for designing electrochemical switches.

Acknowledgements

Partial support of FONDECYT (Grant 105 0344), Convenio CSIC-Universidad de Chile, 2005/2006, the Universidad de Chile and the Universidad Tecnológica Matropolitana are gratefully acknowledged.

References

[1] J.L. Atwood, J.E.D. Davies, D.D. Macnicol (Eds.), Inclusion Compounds, Academic Press, 1984.
[2] V. Sánchez, E. Benavente, M.A. Santa Ana, G. González, Chem. Mater. 11 (1999) 2296.
[3] A. Sanchez, Y. Echeverría, C.M. Sotomayor-Torres, G. González, E. Benavente, Mater. Res. Bull. 41 (2006) 1185.
[4] M.S. Whittingham, Prog. Solid St. Chem. 86 (1982) 463.
[5] D. Yoffe, Solid State Ionics 39 (1990) 1.
[6] G. González, H. Binder, Bol. Soc. Chil. Quím. 41 (1996) 121.
[7] G. González, M.A. Santa Ana, E. Benavente, Electrochim. Acta 43 (1998) 1327.
[8] M. Winter, J.O. Besenhard, M.E. Spahr, P. Novák, Adv. Mater. 10 (1998) 725.
[9] J.H. Choy, S.M. Paek, J.M. Oh, E.S. Jang, Curr. Appl. Phys. 2 (2002) 489.
[10] A.S. Golub, V.I. Zaikovskii, N.D. Lenenko, M. Danot, Y.N. Novikov, Russ. Chem. Bull. 53 (2004) 914.
[11] T.M. Wang, W.M. Liu, J. Tian, X. Shao, D.C. Sun, Polym. Compos. 25 (2004) 111.
[12] R. Bissessur, W. White, D.C. Dahn, Mater. Lett. 60 (2006) 248.
[13] E. Benavente, M.A. Santa Ana, F. Mendizábal, G. González, Coord. Chem. Rev. 224 (2002) 87.
[14] M.A. Py, R.R. Haering, Can. J. Phys. 61 (1983) 76.
[15] E. Ruiz-Hitzky, R. Jiménez, B. Casal, V. Manríquez, M.A. Santa Ana, G. González, Adv. Mater. 5 (1993) 738.
[16] G. González, M.A. Santa Ana, E. Benavente, J.P. Donoso, T.J. Bonagamba, N.C. Mello, H. Panepucci, Solid State Ionics 85 (1996) 225.
[17] G. González, M.A. Santa Ana, E. Benavente, J. Phys. Chem. Solids 58 (1997) 1457.
[18] E. Benavente, M.A. Santa Ana, G. González, F. Becker-Guedes, N.C. Mello, H.C. Panepucci, T.J. Bonagamba, J.P. Donoso, Electrochim. Acta 48 (2003) 1997.
[19] P. Vashista, J.N. Mundy, G.K. Sheny, in: S. Basu, W.L. Worrel (Eds.), Fast Ion Transport in Solid, North Holland, Amsterdam, 1979.
[20] W.M.R. Divilgalpitiya, R.F. Frindt, S.R. Morrison, Science 246 (1989) 369.
[21] N. Lara, E. Ruiz-Hitzky, J. Brazilian Chem. Soc. 7 (1996) 193.
[22] P. Joensen, R.F. Frindt, S.R. Morrison, Mater. Res. Bull. 21 (1986) 457.
[23] V. Sánchez, E. Benavente, V. Lavayen, C. O'Dwyer, C.M. Sotomayor Torres, G. González, M.A. Santa Ana, Appl. Surf. Sci. 252 (2006) 7941.
[24] G. González, M.A. Santa Ana, V. Sánchez, E. Benavente, Mol Cryst. Liq. Cryst. 353 (2000) 301.
[25] M.B. Dines, Science (1975) 1210.
[26] S. Golub, I.B. Shumilova, Yu.N. Novikov, J.L. Mansot, M. Danot, Solid State Ionics 91 (1996) 307.
[27] A.F. Danil de Namor, M.A. Llosa Tanco, J.S.Y. Ng, M. Salomon, Pure Appl. Chem. 67 (1995) 1095.
[28] M.A. Santa Ana, E. Benavente, G. González, J. Coord. Chem. 54 (2001) 481.
[29] M.A. Santa Ana, E. Benavente, P. Gómez-Romero, G. González, J. Mater. Chem. 16 (2006) 3107.